Force Characteristic Analysis of PMLSMs for Magnetic Levitation Stage based on 3-Dimensional Equivalent Magnetic Circuit Network

Gyu-Hong Kang, *Member, IEEE,* Jin Hur, *Senior Member*, *IEEE,* Byoung-Kuk Lee, *Member, IEEE,* and Jung-Pyo Hong, *Senior Member*, *IEEE*

Department of Electrical Engineering, Chang-won National University, Changwon, Kyungnam, 641-773, Korea
e-mail: ipmsm@korea.com, jinhur@keti.re.kr, bklee@keri.re.kr, jphong@sarim.changwon.ac.kr

***Abstract*-This paper deals with the effect of lateral force in the Permanent Magnet Linear Synchronous Motor (PMLSM) for the guidance in magnetic levitation stage. In order to analyze not only overhang effect of the PMLSM, but also lateral asymmetry of secondary (mover), 3-Dimensional Equivalent Magnetic Circuit Network (3-D EMCN), considering movement of the secondary in lateral direction is introduced. The current vector control scheme is applied for the analysis of propulsion, levitation, and lateral force in the PMLSM for magnetic levitation stage.**

***Index Terms*—PMLSM, 3-D EMCN, lateral asymmetry, current vector control scheme.**

I. INTRODUCTION

THE Permanent Magnet Linear Synchronous Motor (PMLSM) has been used in industrial application systems, such as automatic convey system, contactless driving, and high precision position control [1]-[3]. The PMLSM is applied for magnetic levitation stage for semi-conductor manufacture equipments, which has no use for guide rail in lateral position control and propulsion.

In the linear motor, especially the PMLSM, there are several additional force components due to structural peculiarity contrary to cylindrical motors except the thrust for propulsion, which are detent force, attraction force, and lateral force. The detent force is developed from the interaction of Permanent Magnet (PM) mmf harmonics and the airgap permeance harmonics due to slotting of an iron core. It makes thrust ripple be happened and the accuracy of speed and position controls be deteriorated [2]-[3]. The second component, the attraction force between stationary and mover, acts as driving resistance in the PMLSM. However, the attraction force can use as the levitation force by controlling the amplitude of current and the current phase angle in magnetic levitation stage, which is not needed in guide rail [4]-[6]. Moreover, the lateral force is generated by lateral leakage flux due to finite length of width. In case of asymmetry between stationary and mover, the thrust and normal force are reduced, but the lateral force is increased and acted as the recovery force of the mover.

The force characteristics, especially the lateral force, of the PMLSM for magnetic levitation stage without guards are very important for its stability in speed and levitation control systems. Furthermore, its lateral displacement by external disturbance produces the pulsations of the levitation force and the thrust and as results of that, the overall performance of the PMLSM becomes deteriorated. Therefore, in the PMLSM for magnetic levitation stage, the lateral characteristic analysis is highly required for the precise design, considering change of the lateral displacement for restoration [1],[3].

To perform such a magnetic field analysis, 2-dimensional analysis cannot consider lateral characteristics. Therefore, in this paper, 3-D Equivalent Magnetic Circuit Network (3-D EMCN) is used to solve detailed field computation. The purpose of this paper is to analyze the lateral force characteristics of the PMLSM using 3-D EMCN, considering lateral offset displacement and determine optimal current phase angle in the controlled magnetic levitation stage.

II. ANALYSIS METHOD OF PMLSM BY USING 3-D EMCN

A. Controlled Current Vector Scheme of PMLSM

Fig. 1 shows a PMLSM for the magnetic levitation as well as the propulsion in a semi-conductor manufacture stage.

The characteristic analysis of the PMLSM is usually modeled on d-q axis plane by controlled current vector [4], [5]. Fig. 2 shows the vector diagram of the controlled PMLSM on d-q axis plane. As shown in Fig. 2, the total airgap flux is modulated by controlled current vector, so that the thrust and attraction force are controlled by current phase angle, γ. The d-q axis currents are expressed by (1) and (2) and the flux linkage considering armature reaction field and thrust are given by (3) and (4).

$$I_d = -I\sin\gamma \tag{1}$$

$$I_q = I\cos\gamma \tag{2}$$

$$\phi_0 = \phi_f + L_d I_d \tag{3}$$

$$F_x = m\frac{\pi}{\tau}(\phi_f I_q + (L_d - L_q) I_d I_q) \tag{4}$$

where m is phase number, τ is pole pitch, ϕ_f is flux linkage due to PM and L_d, L_q are d-q axis inductance.

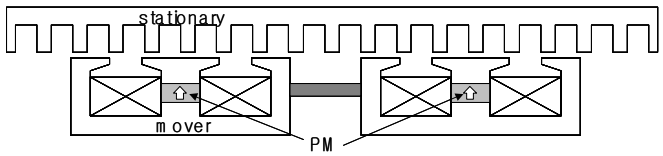

Fig. 1. Structure of PMLSM for magnetic levitation stage.

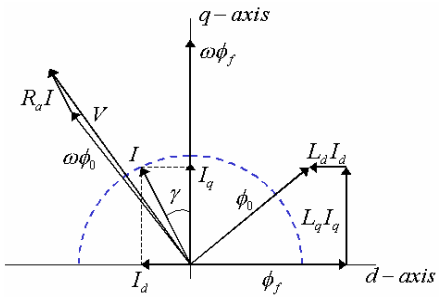

Fig. 2. Vector diagram on d-q axis plane.

B. Analysis Method by 3-D EMCN

A simplified 3-D EMCN model is shown in Fig. 3. 3-D EMCN analysis method divides into elemental volumes of hexahedral shape according to regions and then constructes them by connecting the centroid of adjacent elements with their permeances. The determined y direction permeance, $P^y_{i,j,k}$, by a parallel connection of two related element and magnetic flux are given by (5) and (6). Likewise, the permeances in x and z direction can be calculated by the same way of (5). At each node, the inflow of the magnetic flux is equal to the outflow of it and the magnetic flux continuity condition and system matrix are given by (7) and (8) [1],[3].

$$P^y_{i,j,k} = \frac{\mu_0 \mu_{r1} \mu_{r2} S^y_{i,j,k}}{\mu_0 \mu_{r1} y_{i,j,k} + \mu_0 \mu_{r2} y_{i,j+1,k}} \tag{5}$$

$$\Phi^y_{i,j,k} = P^y_{i,j,k}(U_{i,j+1,k} - U_{i,j,k} + E_{i,j,k}) \tag{6}$$

$$\sum_{n=1}^{6} \Phi_n = \Phi^x_{i-1,j,k} + \Phi^x_{i+1,j,k} + \Phi^y_{i,j-1,k} + \Phi^y_{i,j+1,k} + \Phi^z_{i,j,k-1} + \Phi^z_{i,j,k+1} = 0 \tag{7}$$

$$[\mathbf{P}]\{\mathbf{U}\} = \{\mathbf{F}\} \tag{8}$$

where

$S^y_{i,j,k}$ is area of element between two nodes *(i,j,k)* and *(i,j+1,k)* in y direction

μ is permeability of each elements considering material

$U_{i,j+1,k}$ is unknown magnetic scalar potential of node *(i,j+1,k)*

$E_{i,j,k}$ is MMF of PM or stator winding between two nodes

[P] is permeance coefficient matrix

{U} is matrix of node magnetic scalar potential

{F} is forcing matrix(= permeance × MMF of PM or stator winding

The lateral force is calculated as the derivative of the stored magnetic energy with respect to a small lateral displacement then the lateral displacement of mover is considered by only using information of analysis region without re-modeling and re-meshing the elements. The component of lateral force F_z in direction of the lateral displacement z is as follow [1].

$$F_z = \frac{d W_m}{d z} \tag{9}$$

where W_m is magnetic stored energy in analysis region and z is lateral direction.

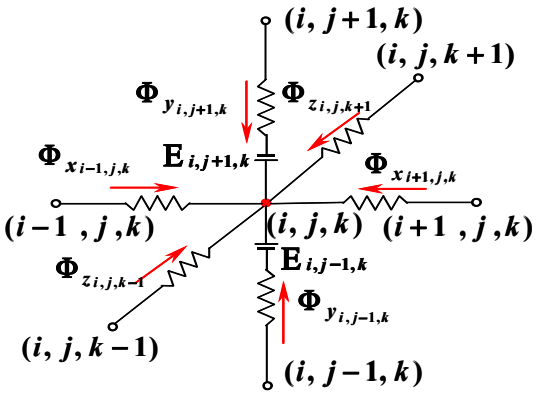

Fig. 3. Configuration of 3-D EMCN and flux flow at a node.

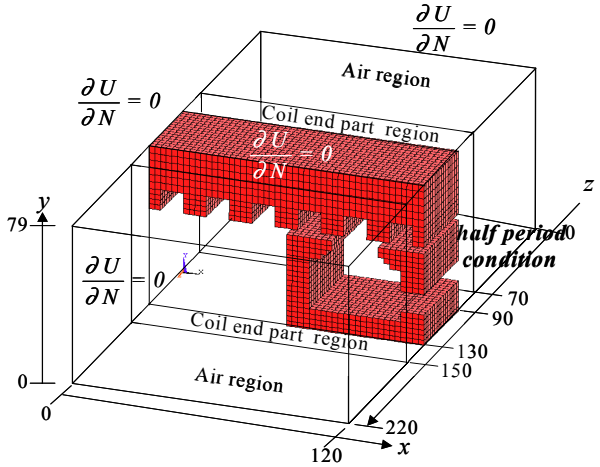

Fig. 4. Analysis model for 3-D EMCN.

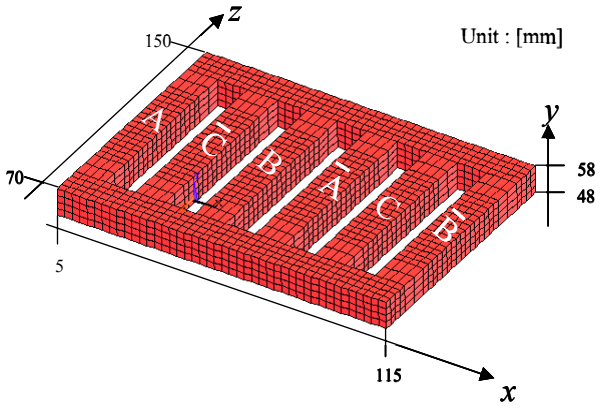

(a) stator winding current distribution

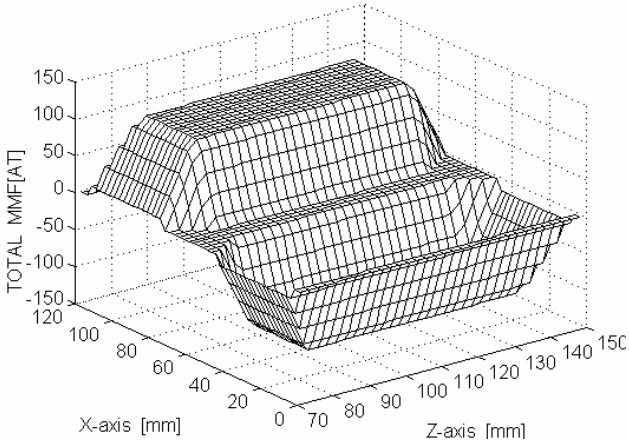

(b) MMF distribution of stator winding current

Fig. 5. Stator winding current distribution for applying 3-D EMCN.

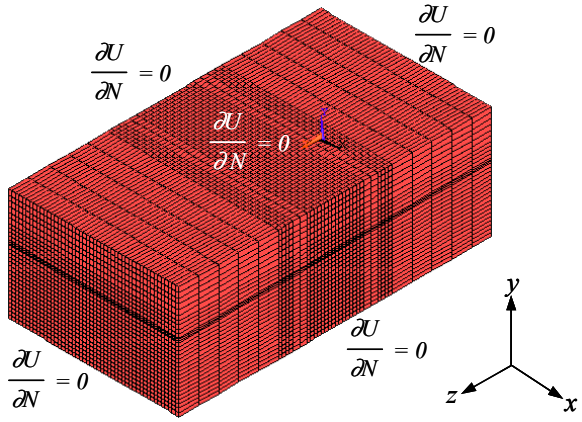

Fig. 6. Boundary condition for applying 3-D EMCN.

Fig. 4 shows analysis model of PMLSM for applying 3-D EMCN with lateral direction (z-axis) length. The analysis region of PMLSM is extended to z-axis for analyzing lateral force considering asymmetry between stationary and mover.

The distribution of stator winding current and MMF are shown in Fig. 5 and Fig. 6 shows boundary condition for 3-D EMCN analysis.

III. Analysis Results

Fig. 7 shows the distribution of the airgap flux density by 3-D EMCN.

Fig. 8 shows the distribution of the flux density vector at *x*-*y* and *y*-*z* plans and compares align and asymmetrical cases of primary and secondary by using 3-D EMCN. In the asymmetrical case, the *z*-direction component of fluxes is generating and lateral force increases due to *z*-direction fluxes.

In magnetic levitation stage by using the PMLSM, the control of position and levitation is performed by not only current amplitude but also controlled current vector like operation of controlled synchronous motor. Therefore, characteristic analysis of PMLSM, such as thrust, levitation force and lateral force for restoration to the original state must be require effect of controlled current vector for precise position control [4]-[5].

Fig. 9 shows thrust and levitation force according to current phase angle γ at align state of primary and secondary. The maximum thrust occurs at current phase angle 0°. In case of the levitation force according to current phase angle, the levitation force increases at a value of controlled current phase angle γ greater than 0°, however, it is reduced at a value of γ less than 0° because d-axis current acts magnetizing filed and (-)d-axis current acts demagnetizing field in the airgap flux. Therefore, in simultaneous propulsion and levitation control of magnetic levitation stage, the control of current vector is strongly required.

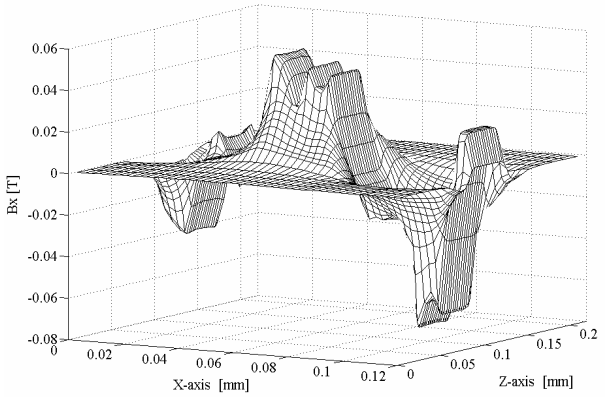

(a) Bx

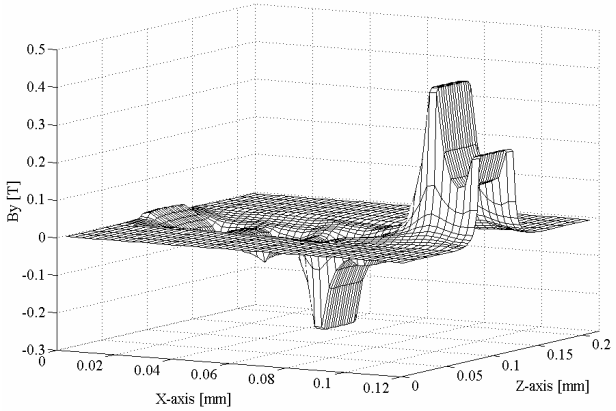

(b) By

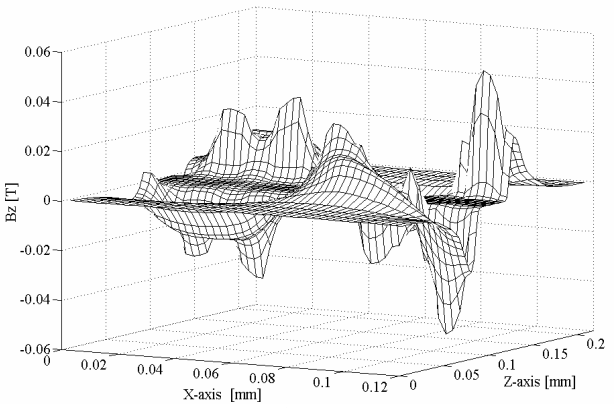

(c) Bz

Fig. 7. Distribution of airgap flux density.

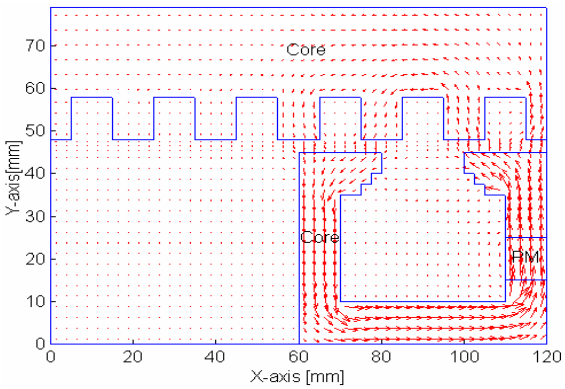

(a) flux distribution in *x*-*y* plane

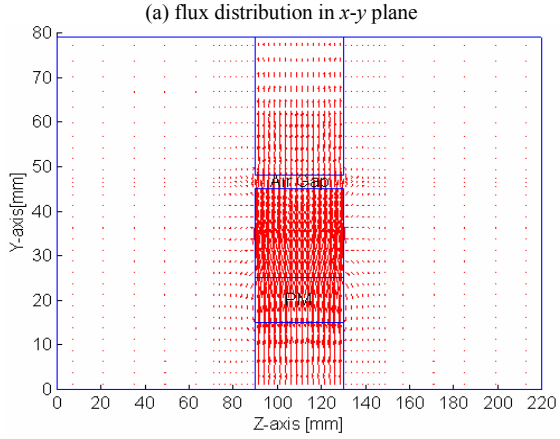

(b) flux distribution in *y*-z plane (offset length = 0mm)

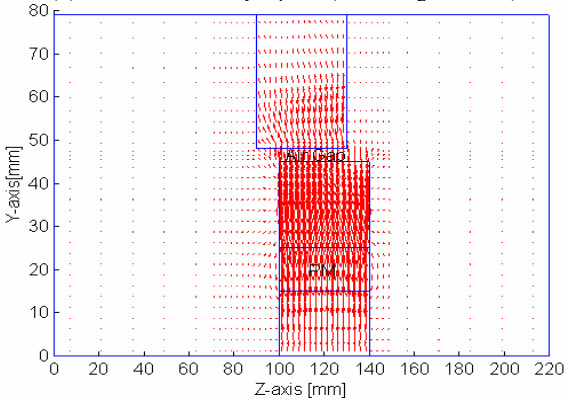

(c) flux distribution in *y*-z plane (offset length = 10mm)

Fig. 8. Flux distribution according to lateral displacement.

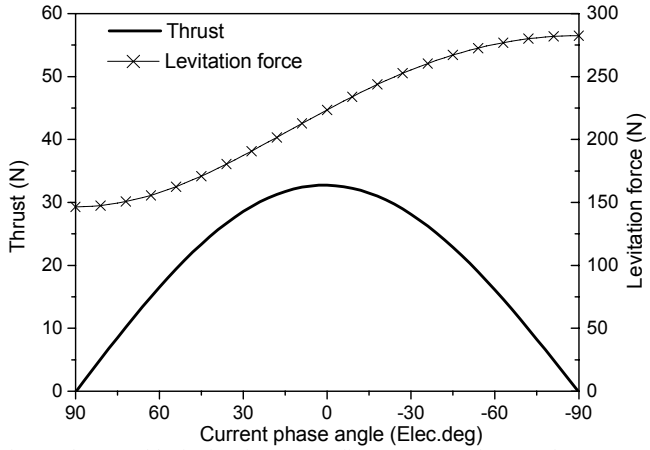

Fig. 9. Thrust and levitation force according to current phase angle.

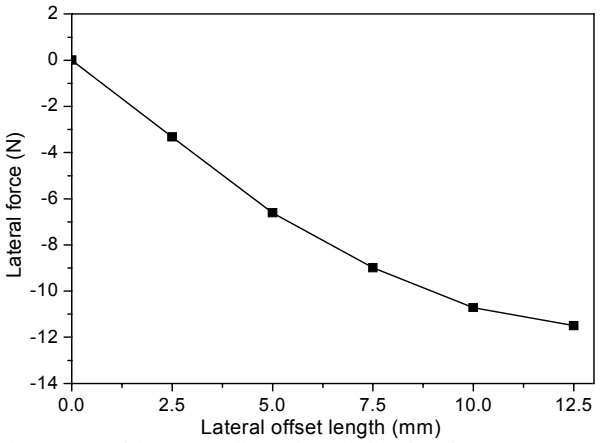

Fig. 10. Lateral force according to lateral offset length.

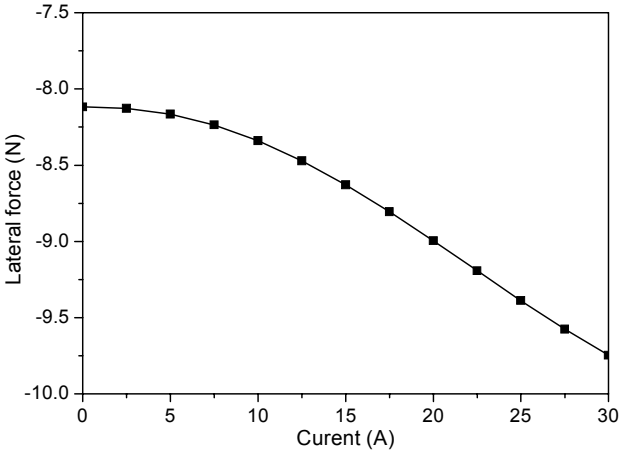

Fig. 11. Lateral force according to current amplitude at 6.5 (mm) offset length.

The lateral force, restoration force, which makes primary and secondary be on the align state is shown in Fig. 10. The lateral force is increased according to the offset length, but the increasing rate is decreased above 7.5 (mm) to offset length.

Fig. 11 shows the characteristics of the lateral force by current amplitude at lateral offset length of 6.5 (mm). In case of only exciting PMs, the generated lateral force is 8.1(N) and

otherwise if the current is applied, total flux increases due to the superposition of flux at the condition of current phase angle 0° on q-axis, resulting in change of the lateral force. Moreover, the lateral force characteristic due to the lateral offset is severely changed by not only current amplitude, but also current phase angle. Because the total airgap flux is changed by d-axis current component. The characteristics of lateral force according to controlled current phase angle at lateral offset length of 6.5 (mm) are shown in Fig. 12. The lateral recovery force is increased when current phase angle is controlled over d-axis.

The surface map of lateral force in accordance with current and current phase angle is shown in Fig. 13. The lateral force is reduced growingly current in a value of γ less than 0°, while on the other the force is increased by more and more current in greater than 0°. It should be notice that the every force is influenced by controlled current phase angle so simultaneous propulsion and levitation control of magnetic levitation stage could by the controlled current phase angle.

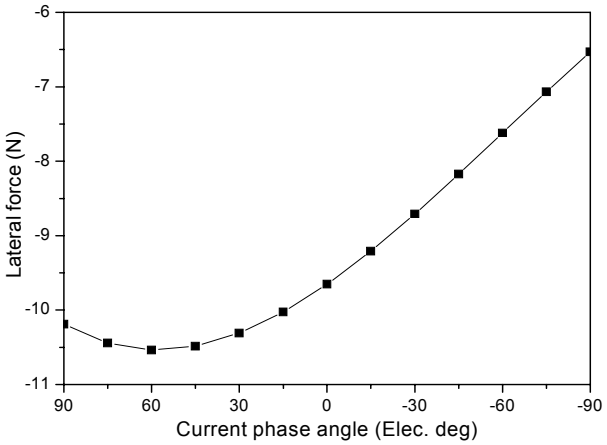

Fig. 12. Lateral force according to current phase angle at 6.5 (mm) offset length.

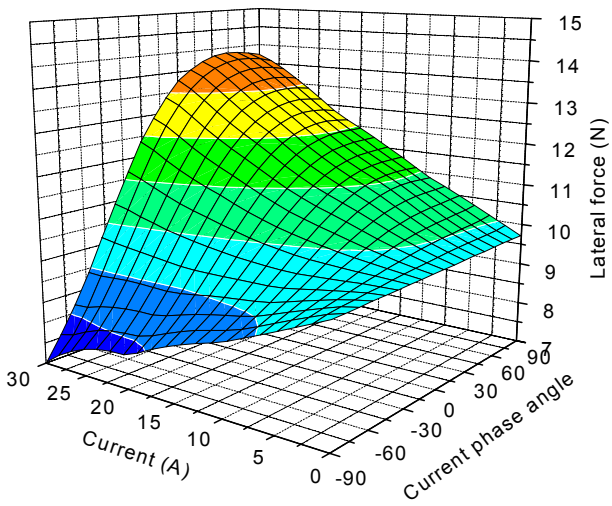

Fig. 13. Lateral force characteristics at 10.0 (mm) offset length.

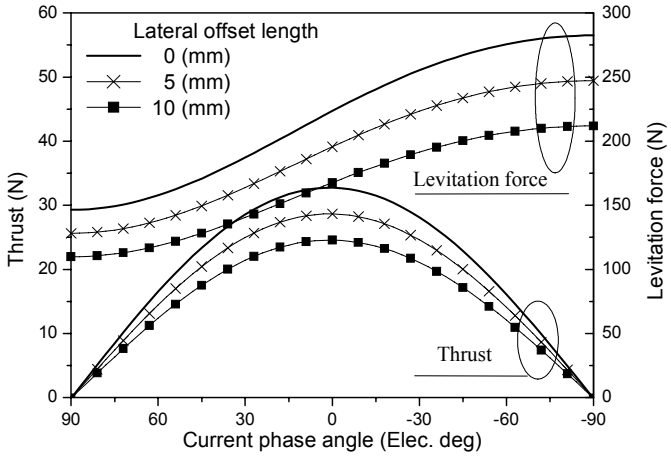

Fig. 14. Force characteristics according to current phase angle.

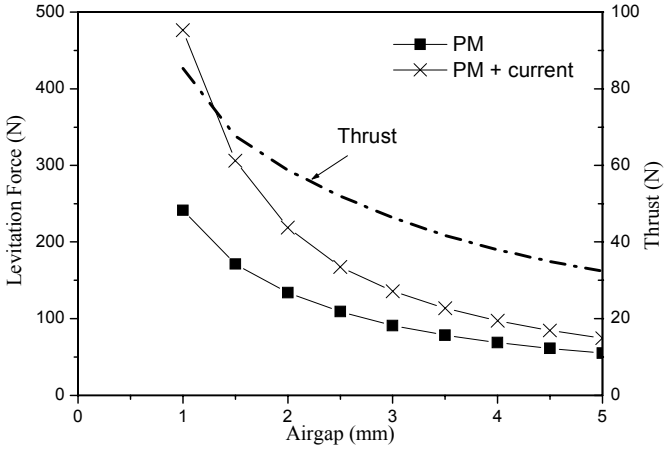

Fig. 15. Force characteristics according to airgap length.

The maximum lateral force occurs at current phase angle 60° while the thrust and the levitation force are decreased. Fig. 14 shows the characteristics of the thrust and the levitation force by controlled current phase angle at lateral offset length of 0 (mm), 5 (mm) and 10 (mm), respectively. It should be noticed that the every force is influenced by controlled current phase angle, so that simultaneous propulsion and levitation control of magnetic levitation stage could be achieved by the controlled current phase angle. Fig. 15 shows the characteristics of the levitation force according to the airgap length, which are in cases of only excited PMs and simultaneously excited PMs and current. In case of simultaneously excited PMs and current, the levitation force occurs greater than the other cases.

IV. CONCLUSION

In this paper, the force characteristic of the PMLSM in magnetic levitation stage is analyzed by using 3-D EMCN and the lateral effect is considered for the force analysis. The force of PMLSM is greatly affected by controlled current phase angle due to the variation of total airgap fluxes.

From these analysis results, one could obtain the trends of thrust, levitation and lateral forces according to lateral asymmetry and controlled current phase angle in the PMLSM without guide-rail system. For simultaneous control system of propulsion and the levitation force, the lateral effect should be analyzed by current phase angle. Based on the presented results, it is highly expected that the analysis results could be effectively used in control scheme of magnetic levitation stage.

REFERENCES

[1] J. Hur, I. S. Jung and D. S. Hyun, " Lateral characteristic analysis of PMLSM considering overhang effect by 3 dimensional equivalent magnetic circuit network method", *IEEE Trans. Magn*., vol. 34, no. 5, pp.3142-3145, Sept. 1998.

[2] I. S. Jung, J. Hur, and D. S. Hyun, "Performance analysis of skewed of PM linear synchronous motor to various design parameters", *IEEE Trans. on Magn*., vol. 37, no. 5, pp.3653-3657, Sept. 2001.

[3] P.J.Hor, Z.Q.Zhu, D.Howe, J.Rees-Jones "Minimization of cogging force in a linear permanent magnet motor", *IEEE Trans. J. Magn*, vol. 34. no. 5, pp. 3544~3547, September. 1998

[4] M. Sanada, S. Morimoto and Y. Takeda, "Interior permanent magnet synchronous motor for high-performance drives", *IEEE Trans. Ind.*, vol. 33, no.4, pp.966-972, July/August 1997.

[5] Gyu-Hong Kang, *et al.*,"Improved parameters modeling of interior permanent magnet synchronous motor by finite element analysis", *IEEE Trans. on Magn*., vol.36, no.4, pp. 1867-1870, July 2000.

[6] R Akmese, J. F. Eastham, "Design of permanent magnet flat linear motors for standstill application" *IEEE Trans.on Magn*, vol. 28, no. 5, pp. 3042-3044, 1992